

A FUNCTIONAL DATA ANALYSIS APPROACH FOR GENETIC ASSOCIATION STUDIES

BY MATTHEW REIMHERR AND DAN NICOLAE

Pennsylvania State University and University of Chicago

We present a new method based on Functional Data Analysis (FDA) for detecting associations between one or more scalar covariates and a longitudinal response, while correcting for other variables. Our methods exploit the temporal structure of longitudinal data in ways that are otherwise difficult with a multivariate approach. Our procedure, from an FDA perspective, is a departure from more established methods in two key aspects. First, the raw longitudinal phenotypes are assembled into functional trajectories prior to analysis. Second, we explore an association test that is not directly based on principal components. We instead focus on quantifying the reduction in L^2 variability as a means of detecting associations. Our procedure is motivated by longitudinal genome wide association studies and, in particular, the childhood asthma management program (CAMP) which explores the long term effects of daily asthma treatments. We conduct a simulation study to better understand the advantages (and/or disadvantages) of an FDA approach compared to a traditional multivariate one. We then apply our methodology to data coming from CAMP. We find a potentially new association with a SNP negatively affecting lung function. Furthermore, this SNP seems to have an interaction effect with one of the treatments.

1. Introduction.

1.1. *The childhood asthma management program.* The childhood asthma management program, CAMP, is a multi-center, longitudinal clinical trial designed to better understand the long term impact of two common daily asthma medications, Budesonide and Nedocromil, on children [The Childhood Asthma Management Program Research Group (1999, 2000)]. Subjects, ages 5–12, with asthma were selected, randomly assigned a particular

Received May 2013; revised August 2013.

Key words and phrases. Functional data analysis, longitudinal data analysis, genome wide association study, functional linear model, functional analysis of variance, hypothesis testing.

This is an electronic reprint of the original article published by the [Institute of Mathematical Statistics](#) in *The Annals of Applied Statistics*, 2014, Vol. 8, No. 1, 406–429. This reprint differs from the original in pagination and typographic detail.

treatment (one of the two drugs or placebo) and monitored for several years. At each clinical visit a number of measurements were taken, but the primary one we focus on here is *forced expiratory volume in one second* or FEV1, which measures the development of the lungs. The goal of the present paper is to associate FEV1, measured longitudinally, with single nucleotide polymorphisms (SNPs) and to detect possible SNP by treatment interactions, while correcting for other covariates such as age and gender. Analyzing longitudinal data can be challenging and often such measurements are converted to scalars where univariate methods can readily be applied [Tantisira et al. (2011)]. However, since the subjects of this study are children, the development of the child over time is also of great interest. This development can be complicated and nonlinear as the child ages, thus, a flexible framework to allow for such patterns is desirable. Conversely, analyzing hundreds of thousands of SNPs requires powerful procedures which exploit any structure inherent in the data. It is reasonable to think that, while a child’s lungs develop “nonlinearly,” their development is still relatively smooth over time, and that major daily fluctuations in FEV1 are primarily noise independent of the underlying development. Finally, while all children make their clinical visits at approximately the same time, the spacing between visits varies throughout the study. So a procedure which is relatively robust against differences in temporal spacing would be vital.

1.2. *Functional data analysis.* Given the nature of the data and our goals, we develop and present a framework for association testing based on functional data analysis. Over the last two decades an abundance of high frequency data and complex longitudinal studies have driven the development of inferential statistical tools for samples of objects which can

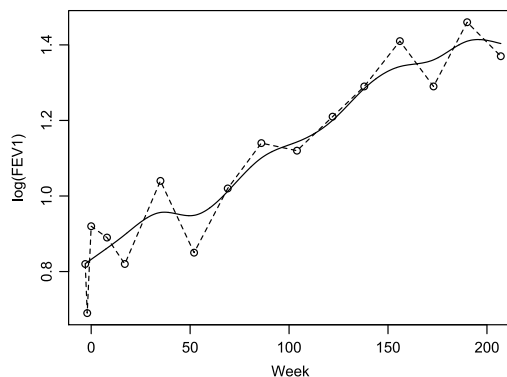


FIG. 1. Plot of one subject from the CAMP study. Circles represent observed values which are linearly interpolated by the dashed line, while the solid line is calculated using smoothing splines.

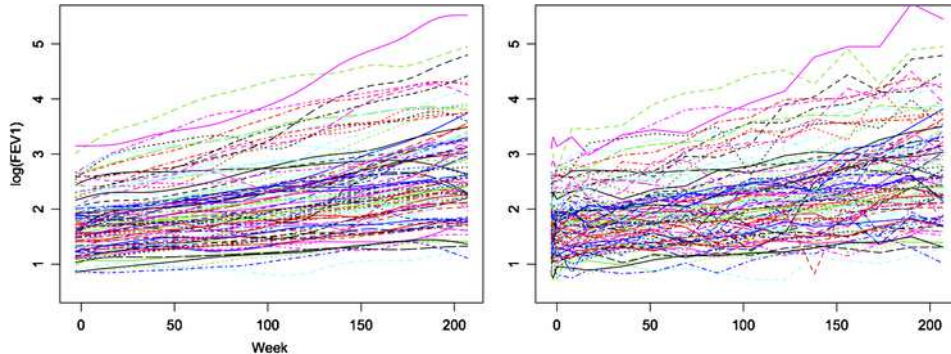


FIG. 2. Plots of the $\log(\text{FEV1})$ curves for the first one hundred subjects. The left panel displays curves obtained via smoothing splines, while the right panel displays curves which are linearly interpolated.

be viewed as functions or trajectories. Tools falling under the umbrella of *functional data analysis* (FDA) have been applied to areas such as human growth patterns [Chen and Müller (2012), Verzelen, Tao and Müller (2012)], gene expression [Tang and Müller (2009)], credit card transaction volumes [Kokoszka and Reimherr (2013)], geomagnetic activity patterns [Gromenko and Kokoszka (2013)], and neuroimaging [Reiss et al. (2011), Zipunnikov et al. (2011)], to name only a few. The driving view in FDA is that certain data structures can be viewed as observations from a function space. To illustrate this point, consider Figure 1. We plot the values of $\log(\text{FEV1})$ for one particular CAMP subject as circles, with linear interpolation indicated by a dashed line. A nonparametric smoother based on B-splines is also plotted as a solid line. As we can see, the B-splines have generated a curve which has smoothed out a lot of the inherent noise in the data, giving a clearer picture of lung development in the child.

We can obtain such a curve for every subject (and actually pool information across children to help generate the curves). We plot the resulting curves for the first 100 CAMP subjects (of 540 total) in Figure 2, alongside their unsmoothed interpolated analogs. We can see that the nonparametric smoothers have decreased the noise inherent in the data, resulting in a clear smooth trajectory for each child's development. Our goal is then to associate the patterns we see in the curves with SNPs and to explore SNP by treatment interactions. However, analyzing such objects is challenging because they are inherently infinite-dimensional objects. The approach we outline here exploits the assumption that the functions come from a Hilbert space by using a *functional linear model* to relate the functional response variables to the univariate covariates. Define $Y_n(t)$ to be the value at time t of the smoothed $\log(\text{FEV1})$ curve for the n th subject. We then use the

following linear model,

$$(1) \quad Y_n(t) = \alpha(t) + \sum_{j=1}^J \beta_{1,j}(t) X_{1;j,n} + \sum_{k=1}^K \beta_{2,k}(t) X_{2;k,n} + \varepsilon_n(t)$$

for $n = 1, \dots, N$, where N is the total number of subjects, and the total number of covariates is $J + K$. Here the $\{Y_n\}$, $\{X_{1;j,n}\}$ and $\{X_{2;k,n}\}$ are observed. The first set of covariates $\{X_{1;j,n}\}$ will include those we wish to correct for (gender, age, etc.), while the second set will include those covariates we wish to test the nullity of (SNPs, treatment effects, etc.). Therefore, the goal of this paper is test the hypothesis

$$H_0: \beta_{2,k}(t) \equiv 0 \quad \text{for } k = 1, \dots, K.$$

To test if H_0 is true, we propose using the reduction in the sum of squared norms as a testing procedure. Our approach is a kind of functional analog to the reduction in sum of squares used in univariate ANOVA methods. This differs from current FDA approaches which are usually based on principal component analysis and attempt to project the infinite-dimensional problem down to a multivariate problem. As we will note in Section 5, FDA methods based on PCA seem to have nontrivial stability problems which become especially evident when carrying out hundreds of thousands of tests.

While the literature on FDA and functional linear models is quite large, we provide some key references in terms of carrying out hypothesis tests with a functional linear model. Cardot et al. (2003) examine a PCA-based testing procedure for a scalar response/functional covariate model which Kokoszka et al. (2008) extends to the fully functional setting. Antoniadis and Sapatinas (2007) examine a mixed-effects model for the modeling of functional data and utilize a wavelet decomposition approach to carry out inference. Zhang and Chen (2007) analyze the effect of the “smoothing first then inference” approach to handling functional data (like the approach considered presently) and consider an L^2 normed approach for testing the nullity of the covariates in a functional linear model. Finally, Reiss, Huang and Mennes (2010) combine a basis expansion approach for model fitting and a permutation testing approach for local hypothesis testing in a functional linear model which is implemented in the R package `Refund`.

1.3. Alternative methodologies. The application of FDA methods in main stream human genetics research is present but still in its infancy. *Functional mapping* methods [Ma, Cassella and Wu (2002), Wu and Lin (2006)] in genetics are similar in spirit to FDA methods, but, as of yet, have not taken advantage of the full flexibility of FDA methods. In most functional mapping settings very specific shapes for describing the data are instilled in the

models with fairly simple error structures, whereas an FDA approach utilizes nonparametric methods to allow for greater flexibility. More generally, the application of FDA methods to longitudinal data is a very active area of research; see, for example, Fan and Zhang (2000), Yao, Müller and Wang (2005), Hall, Müller and Wang (2006), to name only a few. Typically, FDA approaches for longitudinal data focus on estimation and obtaining principal components which differs with our goal of powerful hypothesis testing.

More traditional longitudinal approaches model the dependence between observations from the same subject by introducing random effects. Such an approach typically assumes a very specific structure for the dependence between observations, but the question of how to carry out the desired hypothesis tests is not solved by introducing mixed effects. One could include fixed effects in the form of polynomial functions over time, but given how the children are developing, it is difficult to say which functions would be most appropriate. Another approach would be to use time series to model the within subject dependence. However, the time points are not evenly spaced, the data is not stationary, and one would still have the problem of how to carry out the hypothesis testing.

1.4. *Overview.* The remainder of the paper is organized as follows. In Section 2 we present our approach based on the reduction of sum of squared norms. We first present the single predictor case for illustrative purposes and conclude with the general case that allows one to correct for covariates, test the nullity of factor variables, or test the nullity of multiple covariates. In Section 3 we explore some of the major differences between our procedure and previous FDA approaches. In particular, we show how the difference can be thought of as a difference in weighting schemes on the scores. This view allows for an entire family of testing procedures by choosing different weights. In Section 4 we present a small-scale simulation study. We show how the smoothness of the underlying functions influences the power of our procedure as compared to a PC-based procedure and a traditional multivariate one. In Section 5 we apply our methods to a genome wide association study on childhood asthma that has proven difficult to analyze using traditional methods. We show that there may in fact be a gene by treatment interaction, but further validation is needed. We conclude the paper with discussion of our results in Section 6. All asymptotic results are provided in Appendix A, while proofs are given in Appendix B.

2. Methodology. To construct the trajectories, we first apply a subject by subject B-splines smoother. Some type of smoothing is useful for the CAMP data due to the inherent noise in spirometer readings. A splines-based smoother is especially useful given the fairly smooth and nearly monotonic structure of the trajectories. The smoothing parameter is chosen by

leave-one-subject-out cross-validation, where we compare the mean of the smoothed curves to the observed points of the left out subject. We then form mean function, covariance function and nugget effect estimates. The final curves are obtained by going back to each subject and kriging the curves using the parameter estimates. Such an approach attempts to better utilize information across subjects to help with curve construction. This differs slightly from the smoothing methods found in the PACE package in MATLAB (2013), as we do not utilize a PCA and we construct curves through multiple refinements as opposed to using scatter plot smoothers. Further details are outlined in Reimherr (2013).

We present our methods in two sections. The first considers a functional response with one univariate quantitative covariate and provides an easier [Introduction](#) to our methods. The second section generalizes the first so that our methods are applicable to a wider range of settings. While we introduce all technical notation below, precise mathematical assumptions, theorems and proofs can be found in Appendices [A](#) and [B](#).

Single predictor. We begin by presenting our procedure for the simpler setting when

$$Y_n(t) = \beta(t)X_n + \varepsilon_n(t)$$

for $n = 1, \dots, N$, where X_n and $Y_n(t)$ are assumed to be centered. This will provide a simpler format for introducing the more technical aspects of FDA tools. We assume that $\{X_n\}$ and $\{\varepsilon_n\}$ are two i.i.d. sequences and independent of each other. Without loss of generality, we will also assume that $t \in [0, 1]$. One could assume that t takes values in any closed interval, but the results will remain the same.

The slope function $\beta(t)$ we will assume to be square integrable:

$$\|\beta\|^2 = \int \beta(t)^2 dt < \infty.$$

We will further assume that $\varepsilon_n(t)$ is square integrable almost surely:

$$\|\varepsilon_n\|^2 = \int \varepsilon_n(t)^2 dt < \infty \quad \text{with probability 1.}$$

Therefore, β and ε_n will take values from the Hilbert space $L^2[0, 1]$ (with probability 1) equipped with the inner product

$$\langle x, y \rangle = \int x(t)y(t) dt.$$

This implies that Y_n also takes values from $L^2[0, 1]$ almost surely. Throughout, when writing $\|\cdot\|$ of a function, we will mean this to be the $L^2[0, 1]$ norm. We will also assume that

$$E[X_n^2] < \infty \quad \text{and} \quad E\|\varepsilon_n\|^2 < \infty.$$

This will imply [Bosq (2000)] that ε_n will have a covariance function $C_\varepsilon(t, s)$ which can be expressed as

$$C_\varepsilon(t, s) = \mathbb{E}[\varepsilon_n(t)\varepsilon_n(s)] = \sum_{i=1}^{\infty} \lambda_i v_i(t)v_i(s).$$

Note that this is simply an application of the spectral theorem. One can view $C_\varepsilon(t, s)$ as the kernel of an integral operator acting on $L^2[0, 1]$, in which case $\{\lambda_i\}$ and $\{v_i\}$ will be the eigenvalues and eigenfunctions, respectively, of the resulting operator. The moment assumptions will imply that

$$\sum_{i=1}^{\infty} \lambda_i < \infty.$$

In functional principal component analysis, the v_i are the functional principal components, while λ_i will correspond to the variability explained by the component. A functional PCA-based approach would involve choosing a small number of v_i and projecting the Y_n onto them. This reduces the infinite-dimensional problem involving Y_n into a multidimensional problem involving the scores $\langle Y_n, v_i \rangle$. Unfortunately, as we will note in Section 5, this can induce stability problems in the resulting inferential tools.

We can use this assumed structure to construct a test statistic to determine if β is the zero function by examining how much the inclusion of the covariate reduces the sum of squared norms of the Y_n :

$$\Lambda = \sum_{n=1}^N \|Y_n\|^2 - \sum_{n=1}^N \|Y_n - \hat{\beta}X_n\|^2,$$

where $\hat{\beta}$ is the pointwise least squares estimator

$$\hat{\beta}(t) = \frac{\sum_{n=1}^N Y_n(t)X_n}{\sum_{n=1}^N X_n^2}.$$

In this simple scenario, the procedure is equivalent to taking $N\|\hat{\beta}\|^2$ as the test statistic; however, for testing the nullity of multiple covariates, Λ has a more natural generalization as we will see in the next section. By Theorem 2 in Section A, if $\beta = 0$, then as $N \rightarrow \infty$,

$$\Lambda \xrightarrow{\mathcal{D}} \sum_{i=1}^{\infty} \lambda_i \chi_i^2(1),$$

where $\chi_i^2(1)$ are i.i.d. chi-squared 1 random variables. Since the $\{\lambda_i\}$ are summable, the above will be $O_P(1)$. If $\beta \neq 0$, then

$$\Lambda = NE[X_1^2]\|\beta\|^2 + O_P(1)$$

as $N \rightarrow \infty$ by Theorem 2. Such a procedure does not have the stability problems inherent in PCA techniques and avoids having to choose the number of components. A minor difficulty arises in working with the limiting distribution under the null which does not have a closed-form expression. However, under our assumptions, the weights $\{\lambda_i\}$ are summable and, in practice, typically decrease extremely quickly. Thus, one may obtain p -values by considering the distribution of

$$\sum_{i=1}^I \lambda_i \chi_i^2(1)$$

for some large value of I . As long as I is reasonably large, the procedure will be robust against the choice. One can estimate the $\{\lambda_i\}$ by using the eigenvalues, $\{\hat{\lambda}_i\}$, of the empirical covariance function:

$$\hat{C}_\varepsilon(t, s) = \frac{1}{N-1} \sum (Y_n(t) - \hat{\beta}(t)X_n)(Y_n(s) - \hat{\beta}(s)X_n).$$

By Theorem 3, the $\{\hat{\lambda}_i\}$ will be close to the $\{\lambda_i\}$, uniformly over i , for large N . Thus, we can use the estimated eigenvalues to compute p -values. While there are several methods for approximating the distribution of weighted sums of chi-squares, we have found the method of Imhof (1961) to work very well even for extremely small p -values which are required in genome wide association studies. Further details and comparisons can be found in Duchesne and Lafaye De Micheaux (2010).

Multiple predictors. In order to test the nullity of multiple predictors, interaction terms or factor variables all while correcting for other covariates, one requires a more general testing procedure than found in the previous section. We now examine the larger model

$$\begin{aligned} Y_n(t) &= \alpha(t) + \sum_{j=1}^J \beta_{1,j}(t)X_{1,j;n} + \sum_{k=1}^K \beta_{2,k}(t)X_{2,k;n} + \varepsilon_n(t) \\ &= \alpha(t) + \mathbf{X}_{1,n}^T \boldsymbol{\beta}_1(t) + \mathbf{X}_{2,n}^T \boldsymbol{\beta}_2(t) + \varepsilon_n(t). \end{aligned}$$

We assume that α , $\{\beta_{1,j}\}$ and $\{\beta_{2,k}\}$ all take values in $L^2[0, 1]$ and that ε_n takes values in $L^2[0, 1]$ almost surely. Define the larger vector $\mathbf{X}_n^T = (1, \mathbf{X}_{1,n}^T, \mathbf{X}_{2,n}^T)$ and assume that $E[\mathbf{X}_n^T \mathbf{X}_n] = \Sigma_X$ exists and has full rank. Assume that $\{\mathbf{X}_n\}$ and $\{\varepsilon_n\}$ are two i.i.d. sequences and independent of each other. As before, assume that $\{\varepsilon_n\}$ are centered and that $E\|\varepsilon_n\|^2 < \infty$.

In terms of matrices, the model can be expressed as

$$\mathbf{Y}(t) = \mathbf{X}_1 \boldsymbol{\beta}_1(t) + \mathbf{X}_2 \boldsymbol{\beta}_2(t) + \boldsymbol{\varepsilon}(t),$$

where we group the intercept into the first matrix of covariates. We abuse notation slightly as \mathbf{X}_1 also refers to first observation, but, given the context, it will always be clear what we mean. We define the corresponding least squares estimators

$$\hat{\boldsymbol{\beta}}_1(t) = (\mathbf{X}_1^T \mathbf{X}_1)^{-1} \mathbf{X}_1^T \mathbf{Y}(t) \quad \text{and} \quad \hat{\boldsymbol{\beta}}(t) = (\mathbf{X}^T \mathbf{X})^{-1} \mathbf{X}^T \mathbf{Y}(t),$$

where

$$\mathbf{X} = (\mathbf{X}_1 \quad \mathbf{X}_2).$$

We define the more general version of our test statistic as

$$\Lambda = \sum_{n=1}^N (\|Y_n - \mathbf{X}_{1,n}^T \hat{\boldsymbol{\beta}}_1\|^2 - \|Y_n - \mathbf{X}_n \hat{\boldsymbol{\beta}}\|^2).$$

By Theorem 4 in Appendix A, under the hypothesis that all of the $\boldsymbol{\beta}_2$ coordinates are zero functions, we have that, as $N \rightarrow \infty$,

$$\Lambda \xrightarrow{D} \sum_{i=1}^{\infty} \lambda_i \chi_i^2(K),$$

where the λ_i are as before, but $\chi_i^2(K)$ now have K degrees of freedom corresponding to the K covariates we are testing. Under the alternative, we have, by Theorem 4,

$$\Lambda = N \int \boldsymbol{\beta}_2(t)^T \Sigma_{X,2:1} \boldsymbol{\beta}_2(t) + O_P(1),$$

where $\Sigma_{X,2:1}$ is the Schur complement

$$\Sigma_{X,2:1} = \Sigma_{X,22} - \Sigma_{X,21} \Sigma_{X,11}^{-1} \Sigma_{X,12}.$$

The matrix $\Sigma_{X,2:1}$ appears since we must take into account how dependent the second set of covariates are on the first. The empirical eigenvalues (defined as before) $\{\hat{\lambda}_i\}$ can again be used for computing p -values by Theorem 5.

3. A unified framework. To better understand the difference between our approach and an FDA approach based on principal components [Cardot et al. (2003), Kokoszka et al. (2008)], we provide a more general testing framework that includes both.

Consider the single predictor case. In a traditional FDA approach, one would usually do the following. Using the observations $\{Y_n\}$, form the estimated eigenvalues and eigenfunctions $\{\hat{\lambda}_i, \hat{v}_i\}$ and assume the $\{X_n\}$ have been standardized such that

$$N^{-1} \sum_{n=1}^N X_i = 0 \quad \text{and} \quad N^{-1} \sum_{n=1}^N X_n^2 = 1.$$

Computing the eigenelements is easily done using the FDA package in `R` or `Matlab`; see Ramsay and Silverman (2005) for more details. Then form the test statistic as

$$\Lambda_2 = \sum_{i=1}^I \frac{N^{-1}(\sum_{n=1}^N X_n \langle Y_n, \hat{v}_i \rangle)^2}{\hat{\lambda}_i}.$$

In other words, one computes the covariance between the covariate and each PC, then pools the results after standardizing by $\hat{\lambda}_j$. We can also express

$$\Lambda_2 = \sum_{i=1}^I \frac{N^{-1}(\sum_{n=1}^N X_n \langle Y_n, \hat{v}_i \rangle)^2}{\hat{\lambda}_j} = \sum_{i=1}^I \frac{N \langle \hat{\beta}, \hat{v}_i \rangle^2}{\hat{\lambda}_i}.$$

When $\beta = 0$, Λ_2 is asymptotically $\chi^2(I)$.

Conversely, in this simpler scenario, our Λ test statistic becomes

$$\Lambda = N \|\hat{\beta}\|^2.$$

By Parseval's identity, we have

$$N \|\hat{\beta}\|^2 = N \sum_{i=1}^N \langle \hat{\beta}, \hat{v}_i \rangle^2.$$

So the difference between the two approaches in this simple case can be thought of as a difference in weighting schemes. For the more general case, it helps to think in terms of explained variability. Define

$$\Lambda(\mathbf{w}_N) = N \sum_{i=1}^N w_N(i) \hat{R}_i^2,$$

where \hat{R}_i^2 is the proportion of variance in the i th PC explained by the covariates:

$$\hat{R}_i^2 = \frac{\sum_{n=1}^N (\langle Y_n, \hat{v}_i \rangle - \langle Y_n - X_n \hat{\beta}, \hat{v}_i \rangle)^2}{\sum_{n=1}^N \langle Y_n, \hat{v}_i \rangle^2} = \frac{\langle \hat{\beta}, \hat{v}_i \rangle^2}{\hat{\lambda}_i}.$$

Then Λ_2 corresponds to taking

$$w_N(i) = 1_{1 \leq i \leq I},$$

while Λ corresponds to taking

$$w_N(i) = \hat{\lambda}_i.$$

Put in words, each scheme assigns different weights to the projections. In the traditional case, all (standardized) projections are given equal weights, while in our approach each (standardized) projection is weighted by the

corresponding amount of variability it explains. Both weighting schemes arise naturally, but there might be other meaningful choices of \mathbf{w}_N as well.

Choosing an “optimal” weighting scheme is complicated by the fact that the PCs must be estimated and it is well known that eigenfunction estimates can be very noisy as one moves beyond the first few PCs. Furthermore, while Λ can be expressed using PCA for comparison purposes, it does not directly depend on it, which avoids potential stability problems when dealing with PCs corresponding to small eigenvalues.

4. Simulation study. We carry out a small-scale simulation study to analyze the power of our procedure as compared to other methods. We generate data using the model

$$Y_n(t) = \beta(t)X_n + \varepsilon_n(t).$$

The X_n represent a common SNP with minor allele frequency 0.5 and are taken to be i.i.d. binomial random variables with success parameter 1/2 and trial parameter 2, centered by their mean (in this case 1). The ε_n are generated as stationary, isotropic, Gaussian processes with mean zero and covariance coming from the Matérn class with parameters $(0, 1, 0, 1/4, 5/2)$, representing mean, variance, nugget, scale and ν , respectively, where ν controls the smoothness of the process. In what follows, similar results are obtained if the ε_n are replaced with rougher Matérn processes or Brownian motion (tables available upon request). Such a process will have sample paths which are one time continuously differentiable. The covariance function can be expressed explicitly as, for $t, s \in [0, 1]$ and $d = |t - s|$,

$$E[\varepsilon_n(t)\varepsilon_n(s)] = C(d) = \left(1 + \frac{\sqrt{5}d}{1/4} + \frac{5d^2}{3/16}\right) \exp\left(-\frac{\sqrt{5}d}{1/4}\right).$$

We take $N = 200$, use 1000 repetitions in all cases, and let $M = 5, 10, 20, 50$, where M is the number of points sampled per curve. We assume that the points are always sampled on an even grid on the $[1/M, 1]$ interval and the curves are reconstructed using the same approach mentioned at the beginning of Section 2. We compare three different slope functions:

1. Linear Function: $\beta(t) = 0.18 \times 2(t - 1/2)/0.5773$,
2. Normal CDF: $\beta(t) = 0.18 \times \Phi(7.5(t - 1/2))/0.6517$,
3. Sinusoidal: $\beta(t) = 0.18 \times \sqrt{2} \cos(2\pi t)$.

Notice that the functions are normalized such that the L^2 norm of the function is 0.18, which was chosen to get a clear comparison of power between the procedures. We are especially interested in the second, as we believe its shape to be more reflective of the types of patterns we expect to see in our asthma data as well as human growth data in general; over the course of

several years children grow in spurts followed by a leveling off as they get closer to adulthood. Plots of the above functions are given in Figure 3.

The methods we compare in each scenario are as follows:

- L2: Our Method (\circ),
- PC: A MANOVA performed with 3, 4, and total 5 PCs, the p -value is then taken as the largest (\triangle),
- PC5: A MANOVA performed with 5 PCs (\times),
- MV: A MANOVA performed on the observed points ($+$).

In parenthesis we include the plotting symbol for each procedure plotted in Figure 4. We include both Methods PC and PC5 to illustrate the consequences of having to choose the number of PCs. Method PC is common when trying to determine if one's results are robust against the number of PCs chosen. Note that Methods L2, PC5 and MV are well calibrated, while Method 2 is conservative (tables available upon request, not shown here for brevity).

The results are summarized in Figure 4. There are a few interesting patterns that become clear upon examination. The first is that the PC5 method does quite well in all of the settings. However, the PC method does a bit worse, as expected. This reflects the price of having to choose the number of PCs. Our procedure's behavior is fairly consistent across scenarios due to the normalization of the β functions. The smoothness of the process seems to help our method, and in the normal c.d.f. setting we seem to do quite well, while in the sinusoidal case our method performs slightly worse. The MV method seems to not work as well when compared to the FDA methods. It is especially interesting to see that the multivariate approach does worse

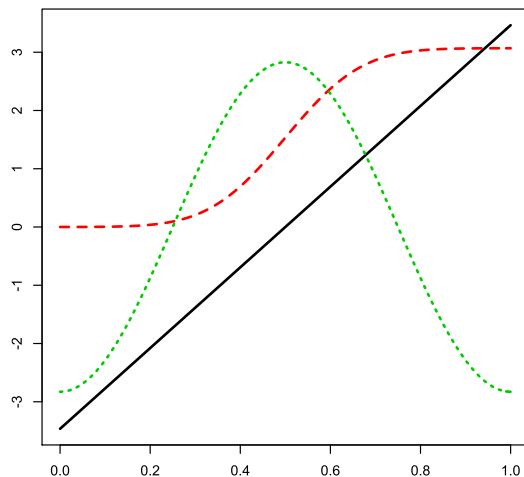


FIG. 3. Plots of the three β functions used under the alternative hypothesis.

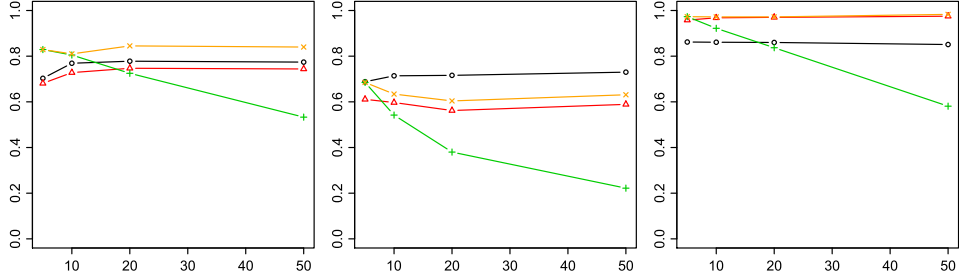


FIG. 4. Power plots for 4 procedures plotted against the number of points sample per curve (M). Method L2 is \circ , PC is \triangle , PC5 is \times , and MV is $+$. The left, middle and right panels correspond to the linear, normal c.d.f. and sinusoidal signals.

as one adds points. This is due to the high dependence of the points across time; increasing the number of points increases the dimension, while the high correlation between points means the overall signal does not increase much.

We conclude this section with a closer examination of what is driving the simulation results. Given the exposition in Section 3, we can gain insight by looking at the R^2 for each PC. That is, we project the Y_n onto each PC and in each case look at what proportion of the variability is explained by the covariate. In Figure 5 we plot the theoretical R^2 values against the PCs.

As we can see, the patterns provide a nice reflection of the power results. For the normal setting, the R^2 decreases with the PC number, while in the sinusoidal setting one gets a peak at PC number 3 (because here β closely matches the 3rd PC). The linear setting has a very interesting alternating pattern (due to the PCs alternating as even/odd functions). When looking at plots of $\langle \beta, v_j \rangle^2$ only (not shown here for brevity), one sees similar patterns, but they are more subtle. It is not until those plots are scaled by the eigenvalues that you see these very strong patterns. An important note is

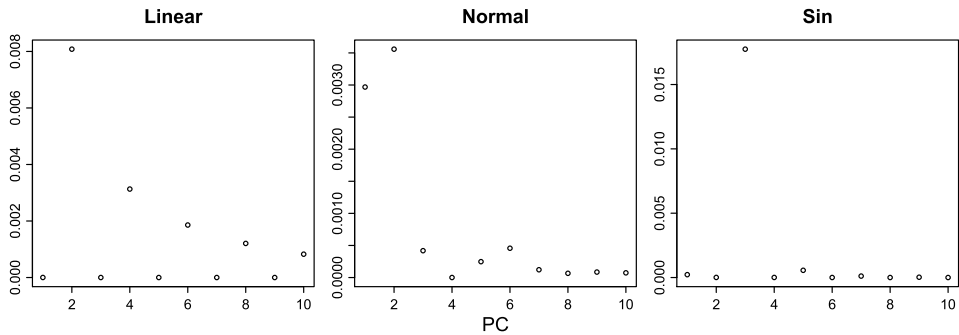


FIG. 5. R^2 plotted against PC number.

that to obtain a similar looking plot empirically, that is, using empirical R^2 values, one needs a rather large sample size. For $N = 200$, one will obtain a very chaotic plot. It is not until N is over 1000, or better yet 10,000, that one sees the empirical plots agreeing nicely with the theoretical ones. This is in large part due to the difficulty in estimating eigenfunctions. Eigenvalues are, in some sense, much easier to estimate accurately. However, the accuracy of eigenfunction estimates depends greatly on what the eigenvalues are, and, in particular, how large and spread out the values are. The smaller an eigenvalue is, and the closer it is to another eigenvalue, the harder the corresponding eigenfunction becomes to estimate.

5. Application. The childhood asthma management project, CAMP, is a multi-center, longitudinal clinical trial designed to better understand the long-term impact of several treatments for mild to moderate asthma [The Childhood Asthma Management Program Research Group (1999, 2000)]. Subjects, ages 5–12, with asthma were selected, randomly assigned a particular treatment and monitored for several years. Our data consists of 540 Caucasian subjects monitored for 4 years, each of whom made 16 clinical visits. Genome-wide SNP data and phenotype information were downloaded from dbGaP (<http://www.ncbi.nlm.nih.gov/gap>) study accession phs000166.v2.p1. Each subject’s first three visits are 1–2 weeks apart and occur prior to treatment; the second two visits are 2 months apart, while the remaining 11 visits are around 4–5 months apart. While a large number of measurements are taken, we focus on the log of *forced expiratory volume in one second* (FEV1), that is, the total volume of air a subject can force out of their lungs in one second. Each subject is given one of two treatments, Budesonide and Nedocromil, or assigned to the Placebo group. Each treatment was assigned to approximately 30% of the subjects, with the remaining 40% receiving the placebo. Trajectories were assembled using a smoothing approach based on B-splines, the details of which can be found in Reimherr (2013).

For each subject we have approximately six hundred and seventy thousand SNPs genotyped after filtering out those with minor allele frequencies below 5%. We used our procedure to test for an association between FEV1 and each SNP, while correcting for age, gender and treatment. The model is given by (at each time point)

$$\log(\text{FEV1}) \sim \text{age} + \text{gender} + \text{treatment} + \text{SNP},$$

where we take age to be the age of the patient at the beginning of the study. A Manhattan plot summarizing all the p -values across chromosomes is given in Figure 6 and a QQ-plot on the \log_{10} scale is given in Figure 7. Examining the QQ-plot, we can see that the procedure is well calibrated, as the p -values smaller than 0.001 fall directly on the 45 degree line, while there are also

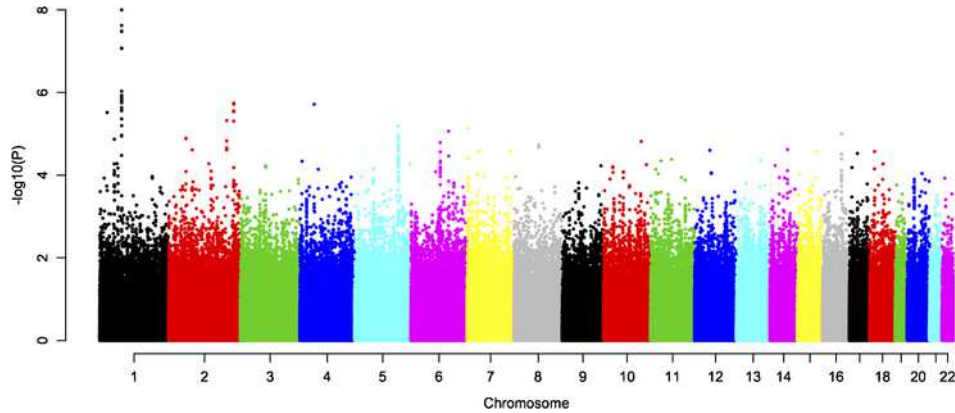


FIG. 6. *Manhattan plot of GWAS p-values across chromosomes.*

some very small p -values indicating some genetic associations. We found one SNP with a p -value of 1.016×10^{-8} : $rs12734254$ in gene $ST6GALNAC5$ on chromosome 1 (significant at the 5% significance level with a Bonferroni correction). A plot of the estimated coefficient function is given in Figure 8. As we can see, presence of the minor allele (frequency 41.63%) is associated with a decrease in lung function which worsens with time. The magnitude of the p -value remained the same for different levels of smoothing in the

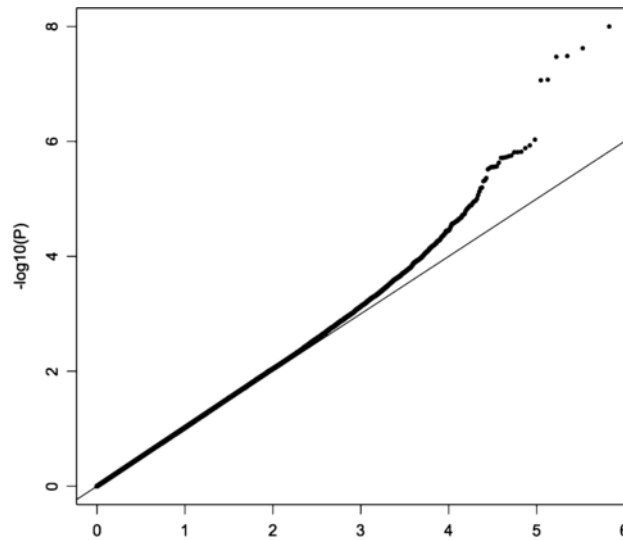


FIG. 7. *QQ-plot comparing GWAS p-values (y-axis, observed) to uniform distribution (x-axis, expected) on \log_{10} scale.*

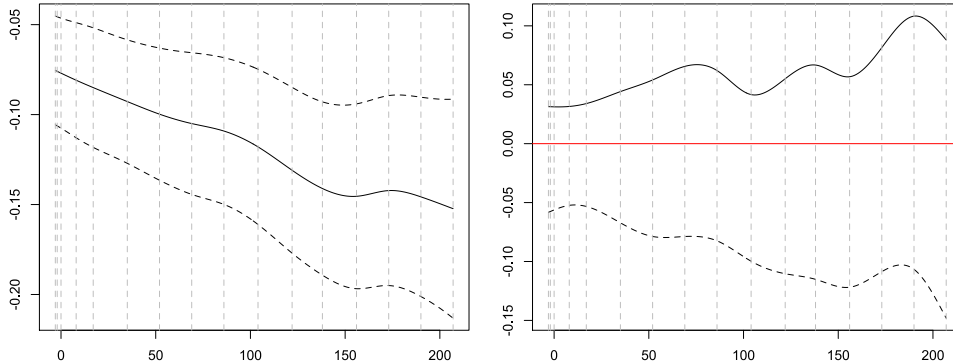


FIG. 8. The left panel is a plot of the SNP (*rs12734254*) effect with pointwise confidence intervals included as dashed lines. The right panel is a plot of the SNP by treatment interaction with Placebo set as the baseline (in red), Budesonide is given by the solid line, and Nedocromil as the dashed. We include grey vertical lines indicating the time of the visits.

preprocessing step, thus, the finding is fairly robust against the initial level of smoothing.

Next, we tested if that SNP also had an interaction effect with treatment; we found a p -value of 0.00284. Since we used significance of the main effects as type of screening before testing for an interaction (which resulted in one test), we do not need to make a correction for multiple testing and, thus, the p -value gives strong evidence that there is a SNP by treatment interaction. In Figure 8 we plot the SNP by treatment interaction effect so that we can better understand the nature of the interaction (with the placebo group set as the baseline). As we can see, the interaction seems to be driven by the difference between the Budesonide group and the Nedocromil group. The Nedocromil group has a stronger decreasing trend, while the Budesonide effect is actually positive. Thus, the presence of the minor allele suggests that Budesonide might in fact have a positive impact on lung function or that at least Budesonide can counter the effects of the deleterious SNP.

To illustrate the power gained by using the FDA approach, we compared it to a univariate approach. If instead of using our approach we take the difference between the endpoints and perform the same type of association analysis (but now with a scalar response), the p -value for our SNP effect becomes 0.002 and the p -value for the interaction test becomes 0.135. Since this is our top SNP, we would expect the p -value for the scalar approach to be smaller, but the drop in p -value is still quite large. More generally, one does not need an FDA approach to exploit the temporal structure in longitudinal data, but it does give a natural framework in which to do it. The potential power gains made by meaningfully pooling across coordinates should be a serious consideration in any longitudinal approach.

Finally, we note that when using an FDA approach based on PCA we ran into some interesting stability issues. In particular, we would on occasion see some very large signals coming from a SNP where the rare allele was only present in a few individuals, making the result unreliable and suspicious. Upon closer examination, it seemed as though the PCs corresponding to smaller eigenvalues were the culprit. This was likely due to the inherent noise in those eigenfunctions which may have been driven by a small number of individuals. Typically, this would not obviously be problematic, but when carrying out a GWAS with hundreds of thousands of SNPs it is possible to come upon a SNP present only in those individuals which are driving the smaller PCs.

6. Discussion. We have presented a new method based on functional data analysis for detecting genetic associations with longitudinal variables. FDA methods allow for a flexible framework that exploits the temporal structure of the data which can result in increased power. Two primary advantages of our particular approach over a PCA-based test is that one does not need to choose the number of principal components (while still maintaining excellent power) and the interpretation of the results is not tied to the interpretability of the shapes of the PCs, which can be especially challenging for the nonleading eigenfunctions. Furthermore, we have found our procedure to be substantially more stable than a PC-based method. This became crucial when conducting hundreds of thousands of tests. We showed how the smoothness of the trajectories and underlying parameter functions determine the power of our procedure, as well as traditional PCA-based methods, as compared to a multivariate approach. In particular, our simulations reinforced the current FDA paradigm: the smoother the objects, the greater the advantage of FDA procedures.

We applied our methodology to data coming from the childhood asthma management study (CAMP). We showed how an association test can be carried out which measures the effect of a SNP on a functional object, while correcting for other covariates. We then followed that test up with an interaction test. Interestingly, we found a mildly significant SNP effect with a significant drug by SNP interaction effect. Such results are of great interest due to the impact they can have on choosing treatment courses for patients.

A useful area for improvement would be to develop a method for estimating/incorporating the interpolation error from the preprocessing step. In high frequency settings such an error is typically very small, but in longitudinal settings where one has a relatively small number of observations per subject, the error can be significant. Indeed, for a very small number of points per curve (2–4) the interpolation error would be so large that classical multivariate methods or methods based on pooled nonparametric smoothers

might be more appropriate. Accounting for this error would hopefully help with power and parameter estimation.

We would be excited to see more FDA methodology developed that does not directly depend on PCA. While we have presented a method based on L^2 norms, it would be interesting to see how one could account for processes whose covariance changes substantially over time. We mentioned the idea of standardizing the functions to have unit variance at every time point. However, it is still unclear how one could take into account the covariance between time points. Indeed, it might be desirable to give less weight to temporal regions with high dependence, since they, in some sense, carry less information than regions with lower dependence.

We believe FDA to be a very interesting and promising method for exploiting the temporal structure in longitudinal studies. The problems facing geneticists are quite challenging due to the sheer abundance of noise inherent in their data. To help overcome this noise, researchers are constantly finding new ways of exploiting information and structure. Here we have shown how an FDA method can exploit a temporal structure to achieve better power. Furthermore, the results are still interpretable as we are, in essence, focusing on large scale patterns. Thus, as we saw in our application, we were able to deliver powerful results with interpretable conclusions. While the FDA toolbox is expanding rapidly, very little has been done which tailors FDA techniques for genetic studies. We hope that we have taken a meaningful step in this direction.

APPENDIX A: ASYMPTOTIC RESULTS

In this section we provide the explicit underlying assumptions and asymptotic results which justify the behavior of our procedure under the null and alternative hypotheses.

Single predictor.

ASSUMPTION 1. Assume we have the following relationship:

$$Y(t) = \beta(t)X + \varepsilon(t),$$

where X and ε are random and take values in \mathbb{R} and $L^2[0, 1]$, respectively. Assume that $\beta \in L^2[0, 1]$ and that the following moment conditions hold:

$$EX = 0, \quad E[\varepsilon(t)] = 0, \quad EX^2 < \infty \quad \text{and} \quad E\|\varepsilon\|^2 < \infty.$$

Finally, assume that $(X_1, Y_1), \dots, (X_N, Y_N)$ are i.i.d. copies of (X, Y) .

THEOREM 1. *If Assumptions 1 holds, then*

$$\sqrt{N}(\hat{\beta} - \beta) \xrightarrow{\mathcal{D}} Z,$$

where Z is a mean zero Gaussian process in $L^2[0, 1]$ with covariance operator

$$\frac{\mathbb{E}[\varepsilon \otimes \varepsilon]}{\mathbb{E}[X^2]}.$$

THEOREM 2. *If Assumptions 1 holds and $\beta = 0$, then*

$$\Lambda \stackrel{\mathcal{D}}{\rightarrow} \sum_{i=1}^{\infty} \lambda_i \chi_i^2(1),$$

where $\{\lambda_i\}$ are the eigenvalues of the covariance operator of ε and $\{\chi_i^2(1)\}$ are i.i.d. chi-squared 1 random variables. If $\beta \neq 0$ (in an L^2 sense), then

$$\Lambda = N\mathbb{E}[X^2] \|\beta\|^2 + O_P(1).$$

THEOREM 3. *If Assumption 1 holds, then*

$$\hat{C}_\varepsilon := \frac{1}{N-1} \sum_{n=1}^N (Y_n - X_n \hat{\beta}) \otimes (Y_n - X_n \hat{\beta}) \xrightarrow{P} C_\varepsilon,$$

where convergence occurs in the space of Hilbert–Schmidt operators and, consequently,

$$\sup_{1 \leq i < \infty} |\hat{\lambda}_i - \lambda_i| \leq \|\hat{C}_\varepsilon - C_\varepsilon\| \xrightarrow{P} 0,$$

where $\{\hat{\lambda}_i\}$ are the eigenvalues of \hat{C}_ε . If in addition $\mathbb{E}\|\varepsilon_n\|^4 < \infty$, then

$$\sqrt{N}(\hat{C}_\varepsilon - C_\varepsilon) \stackrel{\mathcal{D}}{\rightarrow} \mathcal{N}(0, \Gamma),$$

where $\Gamma = \mathbb{E}[(\varepsilon_1 \otimes \varepsilon_1 - C_\varepsilon) \otimes (\varepsilon_1 \otimes \varepsilon_1 - C_\varepsilon)]$. Consequently, one has that

$$\sup_{1 \leq i < \infty} |\hat{\lambda}_i - \lambda_i| \leq \|\hat{C}_\varepsilon - C_\varepsilon\| = O_P(N^{-1/2}).$$

Multiple predictors.

ASSUMPTION 2. Assume we have the following relationship:

$$\begin{aligned} Y_n(t) &= \alpha(t) + \sum_{j=1}^J \beta_{1,j}(t) X_{1,j;n} + \sum_{k=1}^K \beta_{2,k}(t) X_{2,k;n} + \varepsilon_n(t) \\ &= \alpha(t) + \mathbf{X}_{1,n}^T \boldsymbol{\beta}_1(t) + \mathbf{X}_{2,n}^T \boldsymbol{\beta}_2(t) + \varepsilon_n(t), \end{aligned}$$

where J and K are fixed integers and $\mathbf{X}_{1,n}, \mathbf{X}_{2,n}$ and ε are random and take values in $\mathbb{R}^J, \mathbb{R}^K$ and $L^2[0, 1]$, respectively. Assume that $\{\beta_{1,j}\}$ and $\{\beta_{2,k}\}$ are elements of $L^2[0, 1]$ and that $\mathbb{E}\|\varepsilon\|^2 < \infty$. Let $\mathbf{X}_n^T = (1, \mathbf{X}_{1,n}^T, \mathbf{X}_{2,n}^T)$ and assume that $\mathbb{E}[\mathbf{X}_n^T \mathbf{X}_n] = \Sigma_X$ exists and has full rank. Last, assume that $\{\mathbf{X}_1, \dots, \mathbf{X}_N\}$ and $\{\varepsilon_1, \dots, \varepsilon_N\}$ are two i.i.d. sequences, independent of each other, and that $\mathbb{E}[\varepsilon_n(t)] = 0$.

THEOREM 4. *If Assumptions 2 holds and $\beta_2 = 0$, then*

$$\Lambda \xrightarrow{\mathcal{D}} \sum_{i=1}^{\infty} \lambda_i \chi_i^2(K),$$

where $\{\lambda_i\}$ are the eigenvalues of the covariance operator of ε and $\{\chi_i^2(K)\}$ are i.i.d. chi-squared K random variables. If $\beta_2 \neq 0$, then

$$\Lambda = N \int \beta_2(t)^T \Sigma_{X,2:1} \beta_2(t) + O_P(1),$$

where $\Sigma_{X,2:1}$ is the Schur complement

$$\Sigma_{X,2:1} = \Sigma_{X,22} - \Sigma_{X,21} \Sigma_{X,11}^{-1} \Sigma_{X,12}.$$

THEOREM 5. *If Assumptions 2 holds, then*

$$\sqrt{N}(\hat{\beta} - \beta) \xrightarrow{\mathcal{D}} \mathcal{N}(0, \Sigma^{-1} C_\varepsilon),$$

where convergence occurs with respect to the product space $(L^2[0, 1])^N$. Furthermore, we have

$$\hat{C}_\varepsilon := \frac{1}{N-1-J-K} \sum_{n=1}^N (Y_n - \mathbf{X}_n \hat{\beta}) \otimes (Y_n - \mathbf{X}_n \hat{\beta}) \xrightarrow{P} C_\varepsilon,$$

where convergence occurs in the space of Hilbert–Schmidt operators and, consequently,

$$\sup_{1 \leq i < \infty} |\hat{\lambda}_i - \lambda_i| \leq \|\hat{C}_\varepsilon - C_\varepsilon\| \xrightarrow{P} 0,$$

where $\{\hat{\lambda}_i\}$ are the eigenvalues of \hat{C}_ε . If in addition $\mathbb{E}\|\varepsilon_n\|^4 < \infty$, then

$$\sqrt{N}(\hat{C}_\varepsilon - C_\varepsilon) \xrightarrow{\mathcal{D}} \mathcal{N}(0, \Gamma),$$

where $\Gamma = \mathbb{E}[(\varepsilon_1 \otimes \varepsilon_1 - C_\varepsilon) \otimes (\varepsilon_1 \otimes \varepsilon_1 - C_\varepsilon)]$. Consequently, one has

$$\sup_{1 \leq i < \infty} |\hat{\lambda}_i - \lambda_i| \leq \|\hat{C}_\varepsilon - C_\varepsilon\| = O_P(N^{-1/2}).$$

APPENDIX B: PROOFS

Since the simpler single predictor scenario is a special case of the more general setting, we will only prove the more general theorems.

PROOF OF THEOREM 4. In matrix form we can express the model as

$$\mathbf{Y}(t) = \mathbf{X}_1 \beta_1(t) + \mathbf{X}_2 \beta_2(t) + \varepsilon(t) = \mathbf{X} \beta(t) + \varepsilon(t).$$

We use the least squares estimators

$$\hat{\boldsymbol{\beta}}(t) = (\mathbf{X}^T \mathbf{X})^{-1} \mathbf{X}^T \mathbf{Y}(t) \quad \hat{\boldsymbol{\beta}}_1(t) = (\mathbf{X}_1^T \mathbf{X}_1)^{-1} \mathbf{X}_1^T \mathbf{Y}(t).$$

We define our test statistic as

$$\Lambda_2 = \sum_{n=1}^N \|Y_n(t) - \mathbf{X}_{1,n}^T \hat{\boldsymbol{\beta}}_1(t)\|^2 - \sum_{n=1}^N \|Y_n(t) - \mathbf{X}_n^T \hat{\boldsymbol{\beta}}(t)\|^2.$$

The sum of squared residuals based on \mathbf{X} can now be expressed as

$$\begin{aligned} & (\mathbf{Y}(t) - \mathbf{X} \hat{\boldsymbol{\beta}}(t))^T (\mathbf{Y}(t) - \mathbf{X} \hat{\boldsymbol{\beta}}(t)) \\ &= (\boldsymbol{\varepsilon}(t) - \mathbf{X}(\mathbf{X}^T \mathbf{X})^{-1} \mathbf{X}^T \boldsymbol{\varepsilon}(t))^T (\boldsymbol{\varepsilon}(t) - \mathbf{X}(\mathbf{X}^T \mathbf{X})^{-1} \mathbf{X}^T \boldsymbol{\varepsilon}(t)) \\ &= \boldsymbol{\varepsilon}(t)^T \boldsymbol{\varepsilon}(t) - \boldsymbol{\varepsilon}(t)^T \mathbf{X}(\mathbf{X}^T \mathbf{X})^{-1} \mathbf{X} \boldsymbol{\varepsilon}(t). \end{aligned}$$

The residuals using only \mathbf{X}_1 can be expressed as

$$\begin{aligned} & \mathbf{Y}(t) - \mathbf{X}_1 \hat{\boldsymbol{\beta}}_1(t) \\ &= \mathbf{X} \boldsymbol{\beta}(t) + \boldsymbol{\varepsilon}(t) - \mathbf{X}_1 (\mathbf{X}_1^T \mathbf{X}_1)^{-1} \mathbf{X}_1^T \mathbf{Y}(t) \\ &= \mathbf{X} \boldsymbol{\beta}(t) + \boldsymbol{\varepsilon}(t) - \mathbf{X}_1 (\mathbf{X}_1^T \mathbf{X}_1)^{-1} \mathbf{X}_1^T \mathbf{X} \boldsymbol{\beta}(t) - \mathbf{X}_1 (\mathbf{X}_1^T \mathbf{X}_1)^{-1} \mathbf{X}_1^T \boldsymbol{\varepsilon}(t) \\ &= \mathbf{X}_2 \boldsymbol{\beta}_2(t) + \boldsymbol{\varepsilon}(t) - \mathbf{X}_1 (\mathbf{X}_1^T \mathbf{X}_1)^{-1} \mathbf{X}_1^T \mathbf{X}_2 \boldsymbol{\beta}_2(t) - \mathbf{X}_1 (\mathbf{X}_1^T \mathbf{X}_1)^{-1} \mathbf{X}_1^T \boldsymbol{\varepsilon}(t). \end{aligned}$$

So the sum of squared residuals is (after expanding and combining like terms)

$$\begin{aligned} & \boldsymbol{\beta}_2(t)^T \mathbf{X}_2^T \mathbf{X}_2 \boldsymbol{\beta}_2(t) + \boldsymbol{\varepsilon}(t)^T \boldsymbol{\varepsilon}(t) - \boldsymbol{\beta}_2(t)^T \mathbf{X}_2^T \mathbf{X}_1 (\mathbf{X}_1^T \mathbf{X}_1)^{-1} \mathbf{X}_1^T \mathbf{X}_2 \boldsymbol{\beta}_2(t) \\ & \quad - \boldsymbol{\varepsilon}(t)^T \mathbf{X}_1 (\mathbf{X}_1^T \mathbf{X}_1)^{-1} \mathbf{X}_1^T \boldsymbol{\varepsilon}(t) + 2 \boldsymbol{\beta}_2(t)^T \mathbf{X}_2^T \boldsymbol{\varepsilon}(t) \\ & \quad - 2 \boldsymbol{\beta}_2(t)^T \mathbf{X}_2^T \mathbf{X}_1 (\mathbf{X}_1^T \mathbf{X}_1)^{-1} \mathbf{X}_1^T \boldsymbol{\varepsilon}(t). \end{aligned}$$

By examining the orders of each of the terms, one can verify that for $\boldsymbol{\beta}_2 \neq 0$ we have

$$\Lambda_2 = N \int \boldsymbol{\beta}_2(t)^T \Sigma_{X,2:1} \boldsymbol{\beta}_2(t) dt + O_P(1).$$

Since Σ_X has full rank, $\Sigma_{X,2:1}$ is positive definite. Therefore, under the alternative we have

$$\Lambda_2 \rightarrow \infty.$$

Under the null $\boldsymbol{\beta}_2 = 0$, the sum of squared residuals becomes

$$\boldsymbol{\varepsilon}(t)^T \boldsymbol{\varepsilon}(t) - \boldsymbol{\varepsilon}(t)^T \mathbf{X}_1 (\mathbf{X}_1^T \mathbf{X}_1)^{-1} \mathbf{X}_1^T \boldsymbol{\varepsilon}(t).$$

Therefore, the reduction in the sum of squared residuals by including \mathbf{X}_2 is given by

$$\begin{aligned} & \boldsymbol{\varepsilon}(t)^T \mathbf{X}(\mathbf{X}^T \mathbf{X})^{-1} \mathbf{X}^T \boldsymbol{\varepsilon}(t) - \boldsymbol{\varepsilon}(t)^T \mathbf{X}_1 (\mathbf{X}_1^T \mathbf{X}_1)^{-1} \mathbf{X}_1^T \boldsymbol{\varepsilon}(t) \\ &= \boldsymbol{\varepsilon}(t)^T [\mathbf{X}(\mathbf{X}^T \mathbf{X})^{-1} \mathbf{X}^T - \mathbf{X}_1 (\mathbf{X}_1^T \mathbf{X}_1)^{-1} \mathbf{X}_1^T] \boldsymbol{\varepsilon}(t). \end{aligned}$$

Using the Hilbert space CLT, we have that

$$N^{-1/2} \mathbf{X}^T \boldsymbol{\varepsilon}(t) \xrightarrow{\mathcal{D}} \mathbf{Z}(t),$$

where $\mathbf{Z}(t)$ is a vector of Gaussian processes that can be expressed as

$$\mathbf{Z}(t) = \Sigma_X^{1/2} \mathbf{Z}'(t),$$

where $\mathbf{Z}'(t)$ is a vector of i.i.d. Gaussian processes with covariance functions $\mathbb{E}[\varepsilon_n(t)\varepsilon_n(s)]$. Therefore, the reduction in the sum of squared residuals (by the continuous mapping theorem and Slutsky's lemma) is asymptotically equal in distribution to

$$\mathbf{Z}'(t)^T \mathbf{A} \mathbf{Z}'(t),$$

where

$$\mathbf{A} = \mathbf{I} - \Sigma_x^{1/2} \begin{pmatrix} \Sigma_{x,11}^{-1} & 0 \\ 0 & 0 \end{pmatrix} \Sigma_x^{1/2}.$$

Notice that \mathbf{A} is in fact a projection matrix with rank

$$\text{rank}(\mathbf{A}) = \text{trace}(\mathbf{A}) = (K + J) - J = K.$$

Therefore, we have that

$$\mathbf{Z}'(t)^T \mathbf{A} \mathbf{Z}'(t) \stackrel{\mathcal{D}}{=} \sum_{k=1}^K Z'_k(t)^2.$$

This implies that the asymptotic distribution of Λ_2 is now a weighted sum of $\chi^2(K)$ random variables. \square

PROOF OF THEOREM 5. We start by showing the asymptotic normality of $\hat{\boldsymbol{\beta}}$. Notice we can express

$$\sqrt{N}(\hat{\boldsymbol{\beta}}(t) - \boldsymbol{\beta}(t)) = \sqrt{N}(\mathbf{X}^T \mathbf{X})^{-1} \mathbf{X}^T \mathbf{Y}(t) = (N^{-1} \mathbf{X}^T \mathbf{X})^{-1} (N^{-1/2} \mathbf{X}^T \mathbf{Y}(t)).$$

By the multivariate law of large numbers,

$$N^{-1} \mathbf{X}^T \mathbf{X} \rightarrow \Sigma_X.$$

By the CLT for Hilbert spaces,

$$\mathbf{X}^T \mathbf{Y} \xrightarrow{\mathcal{D}} \mathcal{N}(0, \Sigma_C).$$

So by Slutsky's lemma,

$$\sqrt{N}(\hat{\boldsymbol{\beta}} - \boldsymbol{\beta}) \xrightarrow{\mathcal{D}} \mathcal{N}(0, \Sigma^{-1}C)$$

as desired.

Next, turning to the estimate of the covariance operator for the error terms, we have

$$\begin{aligned}\hat{C}_\varepsilon &= \frac{1}{N-1-J-K} \sum_{n=1}^N (Y_n - \mathbf{X}_n \hat{\boldsymbol{\beta}}) \otimes (Y_n - \mathbf{X}_n \hat{\boldsymbol{\beta}}) \\ &= \frac{1}{N-1-J-K} \sum_{n=1}^N (\varepsilon_n - \mathbf{X}_n (\hat{\boldsymbol{\beta}} - \boldsymbol{\beta})) \otimes (\varepsilon_n - \mathbf{X}_n (\hat{\boldsymbol{\beta}} - \boldsymbol{\beta})).\end{aligned}$$

Examining the pieces, we have that

$$\sum_{n=1}^N \mathbf{X}_n (\hat{\boldsymbol{\beta}} - \boldsymbol{\beta}) \otimes \varepsilon_n = \sum_{n=1}^N \mathbf{X}_n (\hat{\boldsymbol{\beta}} - \boldsymbol{\beta}) \otimes \varepsilon_n = O_P(1)$$

by combining the convergence rate of $\hat{\boldsymbol{\beta}}$ and the Hilbert space CLT. Next we have

$$\sum_{n=1}^N \mathbf{X}_n (\hat{\boldsymbol{\beta}} - \boldsymbol{\beta}) \otimes \mathbf{X}_n (\hat{\boldsymbol{\beta}} - \boldsymbol{\beta}) = O_P(1)$$

by combining the convergence rate of $\hat{\boldsymbol{\beta}}$ and the multivariate law of large numbers. Therefore, we can conclude

$$\hat{C}_\varepsilon = N^{-1} \sum_{n=1}^N \varepsilon_n \otimes \varepsilon_n + O_P(N^{-1}).$$

We then immediately have that

$$C_\varepsilon \xrightarrow{P} C_\varepsilon$$

by the Hilbert space law of large numbers. Notice that

$$\|\varepsilon_n \otimes \varepsilon_n\|^2 = \int \int \varepsilon_n(t)^2 \varepsilon_n(s)^2 dt ds = \|\varepsilon_n\|^4.$$

Therefore, $\mathbf{E}\|\varepsilon_n\|^4 < \infty$ implies that $\mathbf{E}\|\varepsilon_n \otimes \varepsilon_n\|^2 < \infty$ and by the Hilbert space CLT we can conclude that

$$\sqrt{N}(\hat{C}_\varepsilon - C_\varepsilon) \rightarrow N(0, \Gamma),$$

where

$$\Gamma = \mathbf{E}[(\varepsilon_n \otimes \varepsilon_n - C_\varepsilon) \otimes (\varepsilon_n \otimes \varepsilon_n - C_\varepsilon)].$$

To obtain the final claim, we apply Corollary 4.5 on page 252 of Gohberg, Goldberg and Kaashoek (2003), which gives

$$|\hat{\lambda}_i - \lambda_i| \leq \|\hat{C}_\varepsilon - C_\varepsilon\|.$$

□

REFERENCES

- ANTONIADIS, A. and SAPATINAS, T. (2007). Estimation and inference in functional mixed-effects models. *Comput. Statist. Data Anal.* **51** 4793–4813. [MR2364541](#)
- BOSQ, D. (2000). *Linear Processes in Function Spaces*. Springer, New York. [MR1783138](#)
- CARDOT, H., FERRATY, F., MAS, A. and SARDA, P. (2003). Testing hypotheses in the functional linear model. *Scand. J. Stat.* **30** 241–255. [MR1965105](#)
- CHEN, K. and MÜLLER, H.-G. (2012). Conditional quantile analysis when covariates are functions, with application to growth data. *J. R. Stat. Soc. Ser. B Stat. Methodol.* **74** 67–89. [MR2885840](#)
- DUCHESNE, P. and LAFAYE DE MICHEAUX, P. (2010). Computing the distribution of quadratic forms: Further comparisons between the Liu–Tang–Zhang approximation and exact methods. *Comput. Statist. Data Anal.* **54** 858–862. [MR2580921](#)
- FAN, J. and ZHANG, J.-T. (2000). Two-step estimation of functional linear models with applications to longitudinal data. *J. R. Stat. Soc. Ser. B Stat. Methodol.* **62** 303–322. [MR1749541](#)
- GOHBERG, I., GOLDBERG, S. and KAASHOEK, M. A. (2003). *Basic Classes of Linear Operators*. Birkhäuser, Basel. [MR2015498](#)
- GROMENKO, O. and KOKOSZKA, P. (2013). Nonparametric inference in small data sets of spatially indexed curves with application to ionospheric trend determination. *Comput. Statist. Data Anal.* **59** 82–94. [MR3000043](#)
- HALL, P., MÜLLER, H.-G. and WANG, J.-L. (2006). Properties of principal component methods for functional and longitudinal data analysis. *Ann. Statist.* **34** 1493–1517. [MR2278365](#)
- IMHOF, J. P. (1961). Computing the distribution of quadratic forms in normal variables. *Biometrika* **48** 419–426. [MR0137199](#)
- KOKOSZKA, P. and REIMHERR, M. (2013). Determining the order of the functional autoregressive model. *J. Time Series Anal.* **34** 116–129. [MR3008019](#)
- KOKOSZKA, P., MASLOVA, I., SOJKA, J. and ZHU, L. (2008). Testing for lack of dependence in the functional linear model. *Canad. J. Statist.* **36** 207–222. [MR2431682](#)
- MA, C. X., CASSELLA, G. and WU, R. (2002). Functional mapping of quantitative trait loci underlying the character process: A theoretical framework. *Genetics* **161** 1751–1762.
- MATLAB (2013). *Version 8.1 (R2013a)*. The MathWorks Inc., Natick, MA.
- RAMSAY, J. O. and SILVERMAN, B. W. (2005). *Functional Data Analysis*, 2nd ed. *Springer Series in Statistics*. Springer, New York. [MR2168993](#)
- REIMHERR, M. (2013). Functional data methods for genome-wide association studies. Ph.D. thesis, Chicago, IL.
- REISS, P. T., HUANG, L. and MENNES, M. (2010). Fast function-on-scalar regression with penalized basis expansions. *Int. J. Biostat.* **6** Art. 28, 30. [MR2683940](#)
- REISS, P. T., MENNES, M., PETKOVA, E., HUANG, L., HOPTMAN, M. J., BISWAL, B. B., COLCOMBE, S. J., ZUO, X.-N. and MILHAM, M. P. (2011). Extracting information from functional connectivity maps via function-on-scalar regression. *Neuroimage* **56** 140–148.
- TANG, R. and MÜLLER, H.-G. (2009). Time-synchronized clustering of gene expression trajectories. *Biostatistics* **10** 32–45.
- TANTISIRA, K. G., LASKY-SU, J., HARADA, M., MURPHY, A., LITONJUA, A. A., HIMES, B. E., LANGE, C., LAZARUS, R., SYLVIA, J., KLANDERMAN, B., DUAN, Q. L., QIU, W., HIROTA, T., MARTINEZ, F. D., MAUGER, D., SORKNESS, C., SZEFLER, S., LAZARUS, S. C., LEMANSKE, R. F., PETERS, S. P., LIMA, J. J., NAKAMURA, Y., TAMARI, M. and WEISS, S. T. (2011). Genomewide association between GLCCII and response to glucocorticoid therapy in asthma. *N. Engl. J. Med.* **365** 1173–1183.

- THE CHILDHOOD ASTHMA MANAGEMENT PROGRAM RESEARCH GROUP (1999). The Childhood Asthma Management Program (CAMP): Design, rationale, and methods. *Control. Clin. Trials* **20** 91–120.
- THE CHILDHOOD ASTHMA MANAGEMENT PROGRAM RESEARCH GROUP (2000). Long-term effects of budesonide or nedocromil in children with asthma. *N. Engl. J. Med.* **343** 1054–1063.
- VERZELEN, N., TAO, W. and MÜLLER, H.-G. (2012). Inferring stochastic dynamics from functional data. *Biometrika* **99** 533–550. [MR2966768](#)
- WU, R. and LIN, M. (2006). Functional mapping—How to map and study the genetic architecture of dynamic complex traits. *Nature Review Genetics* **7** 229–237.
- YAO, F., MÜLLER, H.-G. and WANG, J.-L. (2005). Functional data analysis for sparse longitudinal data. *J. Amer. Statist. Assoc.* **100** 577–590. [MR2160561](#)
- ZHANG, J.-T. and CHEN, J. (2007). Statistical inferences for functional data. *Ann. Statist.* **35** 1052–1079. [MR2341698](#)
- ZIPUNNIKOV, V., CAFFO, B., YOUSEM, D. M., DAVATZIKOS, C., SCHWARTZ, B. S. and CRAINICEANU, C. (2011). Functional principal component model for high-dimensional brain imaging. *NeuroImage* **58** 772–784.

DEPARTMENT OF STATISTICS
PENNSYLVANIA STATE UNIVERSITY
STATE COLLEGE, PENNSYLVANIA 16801
USA
E-MAIL: mreimherr@psu.edu
URL: www.personal.psu.edu/mlr36

DEPARTMENTS OF STATISTICS AND MEDICINE
UNIVERSITY OF CHICAGO
CHICAGO, ILLINOIS 60637
USA
E-MAIL: nicolae@galton.uchicago.edu
URL: www.stat.uchicago.edu/~nicolae